Voltage dependence of Hodgkin-Huxley rate functions for a multistage K^+ channel voltage sensor within a membrane

S. R. Vaccaro*
Department of Physics, University of Adelaide, Adelaide, South Australia, 5005, Australia
(Received 7 July 2014; published 14 November 2014)

The activation of a K^+ channel sensor in two sequential stages during a voltage clamp may be described as the translocation of a Brownian particle in an energy landscape with two large barriers between states. A solution of the Smoluchowski equation for a square-well approximation to the potential function of the S4 voltage sensor satisfies a master equation and has two frequencies that may be determined from the forward and backward rate functions. When the higher-frequency terms have small amplitude, the solution reduces to the relaxation of a rate equation, where the derived two-state rate functions are dependent on the relative magnitude of the forward rates (α and γ) and the backward rates (β and δ) for each stage. In particular, the voltage dependence of the Hodgkin-Huxley rate functions for a K^+ channel may be derived by assuming that the rate functions of the first stage are large relative to those of the second stage—$\alpha \gg \gamma$ and $\beta \gg \delta$. For a *Shaker* IR K^+ channel, the first forward and backward transitions are rate limiting ($\alpha < \gamma$ and $\delta \ll \beta$), and for an activation process with either two or three stages, the derived two-state rate functions also have a voltage dependence that is of a similar form to that determined for the squid axon. The potential variation generated by the interaction between a two-stage K^+ ion channel and a noninactivating Na^+ ion channel is determined by the master equation for K^+ channel activation and the ionic current equation when the Na^+ channel activation time is small, and if $\beta \ll \delta$ and $\alpha \ll \gamma$, the system may exhibit a small amplitude oscillation between spikes, or mixed-mode oscillation, in which the slow closed state modulates the K^+ ion channel conductance in the membrane.

DOI: 10.1103/PhysRevE.90.052713 PACS number(s): 87.15.H−, 87.16.Vy, 87.19.ll

I. INTRODUCTION

Based on the measurement of increased Na^+ and K^+ ion channel conductance during a depolarizing voltage clamp of the squid axon membrane, Hodgkin and Huxley (HH) proposed a model of the action potential that accounted for the threshold potential, the refractory period, and the speed of transmission of the impulse [1]. The Na^+ and K^+ ionic conductance was described by activation variables m and n and an inactivation variable h, that each satisfy a first-order rate equation with empirical transition rate functions that depend on the potential difference V across the membrane [1]. It was assumed that the voltage sensitivity of m, n, and h is dependent on the transverse movement of charged gating particles when the electric field within the membrane is changed. The existence of a delay in the increase of the K^+ and Na^+ channel conductance and the transient nature of the Na^+ conductance increase were represented by $g_K \propto n^4$ and $g_{Na} \propto m^3h$. The HH model has been applied to ion channels in cardiac Purkinje fibers [2], toad myelinated neuron [3], gastropod neuron (including an A-type inactivating K^+ channel) [4], and a bursting pacemaker neuron in the mollusc *Aplysia* [5].

The activation variable for the squid axon K^+ channel satisfies a rate equation,

$$\frac{dn}{dt} = \alpha_n - (\alpha_n + \beta_n)n, \tag{1}$$

where the empirical forward and backward rate functions are of the form

$$\alpha_n = \frac{C(V - A)}{1 - \exp[-B(V - A)]}, \tag{2}$$

$$\beta_n = E\exp[-DV], \tag{3}$$

where V is the membrane voltage, and A to E are constants. The HH rate functions α_n and β_n have been successful in describing activation in a wide variety of ion channels because α_n represents the exponential dependence on V for small depolarizations and the almost linear dependence on V for large clamp potentials, and β_n represents the exponential voltage dependence of the rate constant for a large hyperpolarization. The expression for α_n in Eq. (2) may be obtained from a solution to the Smoluchowski equation for the probability density of states of the voltage sensor, when the potential function is linear in the transverse coordinate Z [6,7], and a rate equation for activation may be derived if there is a large diffusion or potential barrier between closed and open states [8]. However, in view of the presence of negative residues on the S2 and S3 segments within the voltage sensing domain (VSD), as well as induced charge at the dielectric boundary of the membrane, the potential function for the S4 sensor is a nonlinear function of Z for each potential V [9,10].

By expressing a cloned *Shaker* IR K^+ channel in *Xenopus* oocytes, contamination with endogenous currents is minimized, and permits a more accurate determination of the ionic and gating currents across the membrane [11]. Assuming that ion channel opening occurs when the voltage sensor in each of the four subunits is activated through two transitions between three states, followed by a cooperative transition, the model accounts for steady state and kinetic activation and deactivation

*svaccaro@physics.adelaide.edu.au

for both ionic and gating currents, the measurement of gating charge of $13e$ per channel during activation, and the rising phase of the gating current observed during a large depolarization.

Each of the four subunits of a voltage-dependent K^+ channel has a voltage-sensing domain with transmembrane segments S1 to S4, and segments S5 to S6 that form the ion-conducting pore domain. The S4 segment moves transversely through a gating pore in response to a change in the potential difference across the membrane and is stabilized by the interaction between its positively charged residues R1 to R4 and negatively charged amino acids on S2 and S3 segments [12,13], and in the activated state, lipid phosphate groups on the membrane surface [14–16]. Metal-ion constraints on the activation process and molecular dynamics simulations have identified at least three transitions between the resting state and activated state of the S4 sensor within a voltage sensing domain of a K^+ ion channel [17–19]. The attached residues of the S4 segment sequentially translocate across a focused membrane field where the hydrophobic residue F^{290} on the S2 segment of the K^+ channel contributes to the energy barrier for transitions [20]. By measuring the effect of mutants on the gating current of the K^+ channel, it has been shown that F^{290} controls the transfer of the arginine R4 across the membrane field during the final gating transition and has a significant effect on deactivation kinetics but only a small effect on activation time [21]. When the hydrophobic residue I287 on the S2 segment or V363 adjacent to the residue R1 on the S4 segment are replaced by the hydrophilic amino acid Thr, the rate of activation of the K^+ channel is increased by a factor of two and is comparable to the activation rate in a Na^+ ion channel [22]. Therefore, the first forward transition during activation and the first backward transition during deactivation are rate-limiting and dependent on the hydrophobicity of residues on adjacent segments in the VSD.

Assuming that the energy of the voltage sensor is dependent on the Coulomb force between positive S4 residues and negative residues on neighboring segments, the electric field within the membrane and the dielectric boundary force on charged residues, the energy of each potential well and, therefore, the equilibrium distribution of gating charge for each voltage may be calculated for both wild-type and mutant *Shaker* K^+ channels, and good agreement with experimental data is obtained by an appropriate choice of the positions of the negative residues and of the other parameter values [9]. The time-dependence of the survival probabilities of the closed states of the voltage sensor during a voltage clamp may be calculated from a solution of Smoluchowski's equation with a potential function that may be derived by application of Poisson's equation to charged residues within a dielectric slab between solvent regions and is in accord with a three-stage empirical model of the ionic and gating currents for a K^+ channel [23,24]. In particular, the voltage dependence of the forward and backward rate functions for each stage may be derived from the asymmetry of the energy barriers determined by the interaction between S4 residues in close proximity to residues on S2 and S3 segments.

In this paper, assuming that the K^+ channel conductance is modulated by a single S4 sensor that activates in two sequential stages, it is shown that if the rate functions satisfy $\delta \ll \beta$, and either $\alpha \ll \gamma$ or $\alpha \gg \gamma$, the master equation that describes the dynamics of a voltage clamp may be reduced to a rate equation with derived forward and backward rate functions that approximate the functions α_n and β_n for a squid axon K^+ channel [1]. A three-stage model of activation of a K^+ channel may be determined that has the same derived rate functions and survival probability $n(t)$ during a voltage clamp as a two-stage model. If $\delta \ll \beta$, and either $\alpha \ll \gamma$ or $\alpha \gg \gamma$, the activation of a K^+ ion channel during an action potential may be described by a rate equation for the open state probability $n(t)$. However, if the rate functions satisfy $\alpha \ll \gamma$ and $\beta \ll \delta$, both low and high frequency components contribute to $n(t)$ during the voltage clamp, and for an appropriate choice of parameters, the ionic current equation and the master equation for K^+ channel activation exhibit a mixed-mode or bursting oscillation.

II. THE VOLTAGE CLAMP OF A MULTISTAGE K^+ CHANNEL SENSOR

It is assumed that a K^+ channel voltage sensor is a Brownian particle that translocates across voltage-dependent barriers between potential wells by absorbing energy from the thermal environment [9]. The solution of the Smoluchowski equation for a square-well approximation to the potential function of the S4 sensor satisfies a master equation [10], and if activation occurs in two stages between three states (see Fig. 1) [11], the occupation probabilities of the closed states n_1, n_2 and the open state n are determined by

$$\frac{dn_1(t)}{dt} = -\alpha n_1(t) + \beta n_2(t), \tag{4}$$

$$\frac{dn_2(t)}{dt} = \alpha n_1(t) + \delta n(t) - (\beta + \gamma) n_2(t), \tag{5}$$

$$\frac{dn(t)}{dt} = \gamma n_2(t) - \delta n(t), \tag{6}$$

where the rate functions

$$\begin{aligned} \alpha(V) &= \alpha_0 \exp[q_\alpha (V - V_0)/kT], \\ \beta(V) &= \beta_0 \exp[-q_\beta (V - V_0)/kT], \end{aligned} \tag{7}$$

$$\begin{aligned} \gamma(V) &= \gamma_0 \exp[q_\gamma (V - V_0)/kT], \\ \delta(V) &= \delta_0 \exp[-q_\delta (V - V_0)/kT], \end{aligned} \tag{8}$$

$\alpha_0, \beta_0, \gamma_0, \delta_0$ are constants (ms^{-1}), q_i is the equivalent charge for each forward or backward transition, k is Boltzmann's constant, $kT/e \approx 25$ mV, e is the electronic charge, V_0 is a constant, and V is the membrane voltage (in mV).

$$n_1 \underset{\beta}{\overset{\alpha}{\rightleftharpoons}} n_2 \underset{\delta}{\overset{\gamma}{\rightleftharpoons}} n$$

FIG. 1. Two-stage activation model of a K^+ ion channel voltage sensor, where the occupation probabilities of the closed states n_1, n_2 and the open state n satisfy a master equation, and α, β, γ, and δ are voltage-dependent rate functions between states.

For a large hyperpolarized holding potential, we may assume that $n_1(0) = 1$, and $n(0) = n_2(0) = 0$, and if the K^+ channel voltage sensor is depolarized to a clamp potential V (activation), the solution of Eqs. (4)–(6) for the open state is (see Appendix A)

$$n_A(t) = \frac{\alpha\gamma}{\omega_1\omega_2} + \frac{\alpha\gamma}{\omega_1(\omega_1-\omega_2)}\exp(-\omega_1 t) - \frac{\alpha\gamma}{\omega_2(\omega_1-\omega_2)}\exp(-\omega_2 t), \quad (9)$$

where ω_1 and ω_2 ($> \omega_1$) are solutions of the characteristic equation

$$\omega^2 - \omega(\alpha+\beta+\gamma+\delta) + \alpha\gamma + \delta(\alpha+\beta) = 0. \quad (10)$$

However, if the S4 sensor is initially in the open state [$n(0) = 1$, and $n_1(0) = n_2(0) = 0$], and if the K^+ channel sensor is repolarized to a clamp potential V (deactivation), the solution is (see Appendix A)

$$n_D(t) = \frac{\alpha\gamma}{\omega_1\omega_2} + \frac{\delta(\omega_2-\gamma-\delta)}{\omega_1(\omega_2-\omega_1)}\exp(-\omega_1 t) + \frac{\delta(\omega_1-\gamma-\delta)}{\omega_2(\omega_1-\omega_2)}\exp(-\omega_2 t). \quad (11)$$

Assuming that the rate functions of the first step are larger than the second step ($\beta \gg \delta$ and $\alpha \gg \gamma$), it may be shown from Eq. (10) that $\omega_1 \approx \gamma\alpha/(\alpha+\beta)+\delta$ and $\omega_2 \approx \alpha+\beta \gg \omega_1$, and Eqs. (9) and (11) become

$$n_A(t) \approx \frac{\alpha\gamma}{\alpha\gamma+\delta(\alpha+\beta)}[1-\exp(-\omega_1 t)], \quad (12)$$

$$n_D(t) \approx \frac{\alpha\gamma+\delta(\alpha+\beta)\exp(-\omega_1 t)}{\alpha\gamma+\delta(\alpha+\beta)}. \quad (13)$$

Equations (12) and (13) are solutions of the rate equation [1]

$$\frac{dn}{dt} = \alpha_{n,2} - (\alpha_{n,2}+\beta_{n,2})n, \quad (14)$$

where

$$\alpha_{n,2}(V) = \frac{\omega_1\alpha\gamma}{\alpha\gamma+\delta(\alpha+\beta)}, \quad (15)$$

$$\beta_{n,2}(V) = \frac{\omega_1\delta(\alpha+\beta)}{\alpha\gamma+\delta(\alpha+\beta)}, \quad (16)$$

and, therefore, $\omega_1 = \alpha_{n,2}+\beta_{n,2}$ and $\beta_{n,2}/\alpha_{n,2} = (1+\beta/\alpha)\delta/\gamma$. Substituting $\omega_1 \approx \gamma\alpha/(\alpha+\beta)+\delta$, we may write

$$\alpha_{n,2}(V) \approx \frac{\gamma}{1+\beta/\alpha}, \quad (17)$$

$$\beta_{n,2}(V) \approx \delta, \quad (18)$$

which provide a good fit to the empirical rate functions α_n and β_n for the squid axon K^+ channel [1] (see Fig. 2). The subscript "n,2" for α and β in Eqs. (17) and (18) denotes a two-stage expression for the K^+ ion channel rate functions, where $\gamma \approx \alpha_n$ for large depolarized potentials, the ratio $\beta/\alpha \approx \gamma/\alpha_n - 1$, and $\delta = \beta_n$. There is also good agreement between the survival probability of the state $n(t)$ during a voltage clamp calculated from a rate equation with α_n and β_n and from the master equation solutions Eqs. (9) and (11) [see Figs. 3(a) and 3(b)], and therefore, an activation process for the voltage sensor with at least two stages provides a physical basis for the mathematical form and asymmetry of α_n and β_n, without assuming a constant electric field within the membrane. The function $\alpha_{n,2}(V)$ has the almost linear variation of $\gamma(V)$ for large depolarizing clamp potentials (as $q_\gamma \approx 0.3e$), and has the exponential variation of $\beta(V)$, as well as $\alpha(V)$ and $\gamma(V)$, for depolarizations near the resting state, whereas $\beta_{n,2}(V)$ has the exponential voltage dependence of $\delta(V)$.

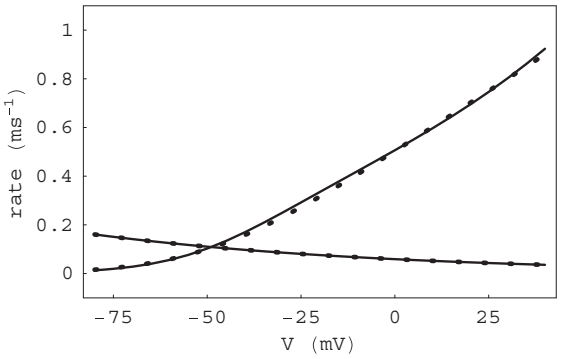

FIG. 2. The derived rate functions $\alpha_{n,2}$ and $\beta_{n,2}$ (solid line) in Eqs. (17) and (18) provide a good approximation to the HH rate functions (ms^{-1}) $\alpha_n = 0.01(V+50)/\{1-\exp[-0.1(V+50)]\}$ and $\beta_n = 0.125\exp[-(V+60)/80]$ (dotted line) when the rate functions for two-stage activation (ms^{-1}) are $\alpha(V) = 6.4\exp[0.3(V-V_0)/25]$, $\beta(V) = 17.6\exp[-1.4(V-V_0)/25]$, $\gamma(V) = 0.24\exp\ [0.345(V-V_0)/25]$, $\delta(V) = 0.125\exp[-0.312(V-V_0)/25]$, $V_0 = -57.9$.

However, if we assume that $\beta \gg \delta$ and $\gamma \gg \alpha$, a limiting case of the description of ionic and gating currents within the *Shaker* K^+ ion channel [11], it may be shown that $\omega_1 \approx$

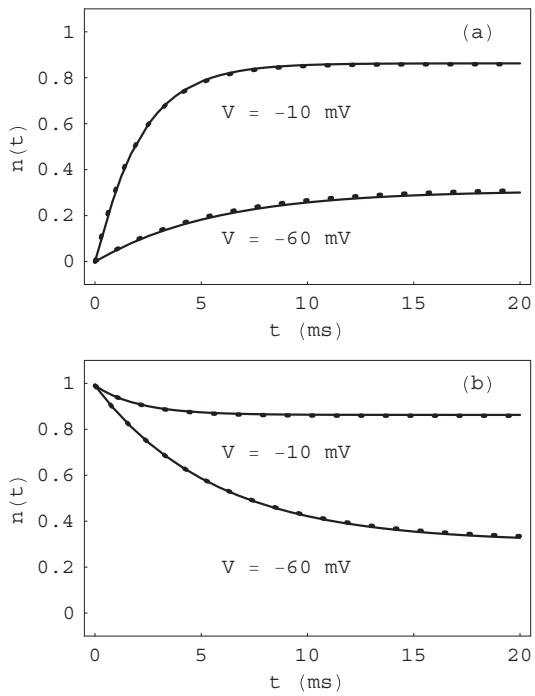

FIG. 3. Survival probability of the state $n(t)$ during a voltage clamp for a two-stage activation model of a K^+ ion channel (solid line) and for the HH squid axon model (dotted line) during (a) activation and (b) deactivation (see Fig. 2).

$\alpha\gamma/(\gamma+\beta)+\delta(\alpha+\beta)/(\gamma+\beta)$ and $\omega_2 \approx \gamma+\beta \gg \omega_1$, and Eqs. (9) and (11) become

$$n_A(t) \approx \frac{\alpha\gamma}{\alpha\gamma+\delta(\alpha+\beta)}[1-\exp(-\omega_1 t)], \tag{19}$$

$$n_D(t) \approx \frac{\alpha\gamma}{\alpha\gamma+\delta(\alpha+\beta)} + \frac{\delta(\gamma-\alpha)\exp(-\omega_2 t)}{(\gamma+\beta)^2} + \frac{\delta(\beta-\delta)\exp(-\omega_1 t)}{(\gamma+\beta)(\alpha+\delta)}, \tag{20}$$

and for a sufficiently large hyperpolarization, $\beta-\delta > \gamma-\alpha$, and we may write

$$n_D(t) \approx \frac{\alpha\gamma+\delta(\alpha+\beta)\exp(-\omega_1 t)}{\alpha\gamma+\delta(\alpha+\beta)}. \tag{21}$$

Equations (19) and (21) are also solutions of Eq. (14), and substituting $\omega_1 = \alpha\gamma/(\gamma+\beta)+\delta(\alpha+\beta)/(\gamma+\beta)$ into Eqs. (15) and (16),

$$\alpha_{n,2}(V) \approx \frac{\alpha}{1+\beta/\gamma} = \frac{\alpha_0 \exp[q_\alpha V/kT]}{1+(\beta_0/\gamma_0)\exp[-(q_\beta+q_\gamma)V/kT]}, \tag{22}$$

$$\beta_{n,2}(V) \approx \frac{\delta(\alpha+\beta)}{(\gamma+\beta)} = \frac{\delta_0 \exp[-q_\delta V/kT](1+(\alpha_0/\beta_0)\exp[(q_\alpha+q_\beta)V/kT])}{1+(\gamma_0/\beta_0)\exp[(q_\gamma+q_\beta)V/kT]}, \tag{23}$$

if $V_0 = 0$. For a large depolarizing potential V, $\alpha_{n,2}(V) \approx \alpha$ and $\beta_{n,2}(V) \approx \delta\alpha/\gamma$, whereas for a hyperpolarizing potential, $\alpha_{n,2}(V) \approx \gamma\alpha/\beta$ and $\beta_{n,2}(V) \approx \delta$, and have a similar form to the empirical rate functions for a delayed rectifier K^+ ion channel in a cardiac Purkinje fiber [25], which may be expressed as

$$\alpha_x = \frac{D\exp[C(V-A)]}{1+\exp[-B(V-A)]}, \tag{24}$$

$$\beta_x = \frac{H\exp[-G(V-E)]}{1+\exp[F(V-E)]}, \tag{25}$$

where A–H are constants. For a *Shaker* K^+ ion channel [11], the derived rate functions $\alpha_{n,2}$ and $\beta_{n,2}$ may be approximated by functions α_H and β_H, which have the same mathematical form as the rate functions α_n and β_n (see Fig. 4). Although there is good agreement for small depolarizations between the survival probability $n(t)$ during a voltage clamp calculated from a rate equation with $\alpha_{n,2}$ and $\beta_{n,2}$, and from Eqs. (9) and (11) [see Figs. 5(a) and 5(b)], for larger depolarizations the higher-frequency component of the solution makes a contribution and therefore deviates from the two-state model. However, if $\beta(V)$ and $\gamma(V)$ are increased by a factor of 3, the rate equation provides a better fit to two-stage activation for larger depolarizations [see Fig. 5(c)].

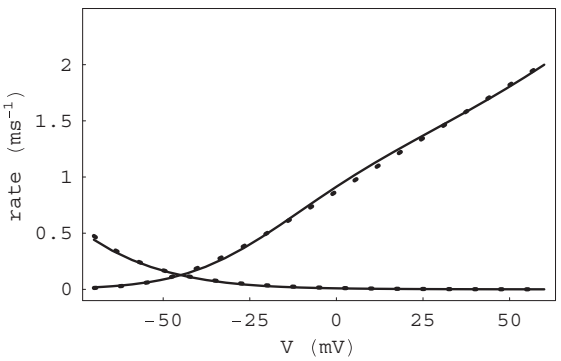

FIG. 4. The derived rate functions $\alpha_{n,2}$ and $\beta_{n,2}$ (solid line) in Eqs. (15) and (16) are calculated for the rate functions determined experimentally for the *Shaker* K^+ ion channel [11] $\alpha(V) = 1.1\exp(0.25V/25)$, $\beta(V) = 0.37\exp(-1.6V/25)$, $\gamma(V) = 2.8\exp(0.32V/25)$, $\delta(V) = 0.021\exp(-1.1V/25)$ (ms^{-1}), and may be approximated by the rate functions $\alpha_H = 0.019(V+45.8)/\{1-\exp[-0.15(V+45.8)]\}$ and $\beta_H = 0.135\exp[-0.052(V+45.8)]$ for single transition activation (dotted line).

If the rate functions satisfy $\beta \ll \delta$ and $\alpha \ll \gamma$, from Eqs. (9) and (10), $\omega_1 \approx \alpha+\beta\delta/(\gamma+\delta) \ll \omega_2 \approx \gamma+\delta$, and

$$n_A(t) \approx \frac{\alpha\gamma}{\omega_1\omega_2} + \frac{\alpha\gamma}{\omega_2}\left[-\frac{\exp(-\omega_1 t)}{\omega_1} + \frac{\exp(-\omega_2 t)}{\omega_2}\right]. \tag{26}$$

The high-frequency term is small for all potentials, and hence

$$n_A(t) \approx \frac{\alpha\gamma}{\alpha\gamma+\delta(\alpha+\beta)}[1-\exp(-\omega_1 t)]. \tag{27}$$

For deactivation, the low-frequency term in Eq. (11) is small, and

$$n_D(t) \approx \frac{\alpha\gamma+\delta(\alpha+\beta)+\delta\omega_1[\exp(-\omega_2 t)-1]}{\alpha\gamma+\delta(\alpha+\beta)}. \tag{28}$$

Therefore, the ionic currents during a voltage clamp cannot be described by a rate equation, and similarly, if $\beta \ll \delta$ and $\alpha \gg \gamma$, the ionic currents have contributions from both low- and high-frequency terms, and therefore require a master equation description.

Although the K^+ ionic current is a function of the activation variable n if the rate functions satisfy $\delta \ll \beta$ and either $\alpha \gg \gamma$ or $\gamma \gg \alpha$, the gating current of the ion channel is composed of a fast component, considered to be a redistribution of the charge of the S4 sensor within energy wells, and a slow component generated by transitions between stationary states. The gating charge $\overline{Q}_i$ associated with the transition to the ith state from the first state is the change in charge induced in the surrounding solvent [26] and may be expressed as $\sum_{j=2}^{i} Q_j$, where Q_j is the gating charge for the transition from the $(j-1)$th state to the jth state. The observable gating charge $Q_g(t)$ for each subunit of the K^+ ion channel is dependent on the survival probability for each state, and if the voltage sensor activates in two steps, $Q_{g,2}(t) = Q_2 n_2(t) + (Q_2+Q_3)n(t)$, and the gating current

$$I_{g,2}(t) = Q_2\frac{dn_2}{dt} + (Q_2+Q_3)\frac{dn}{dt}. \tag{29}$$

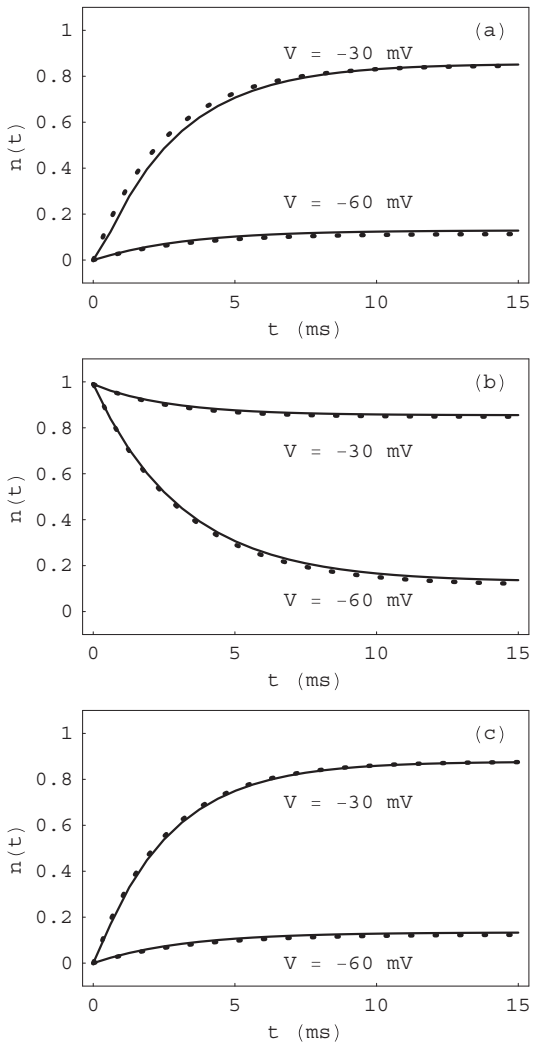

FIG. 5. Survival probability of the state $n(t)$ during a voltage clamp for a two-stage model of a K^+ channel (solid line) and HH model (dotted line) during (a) activation and (b) deactivation, for the rate functions described in the legend of Fig. 4, and (c) activation when $\beta(V)$ and $\gamma(V)$ are increased by a factor of 3, and the rate functions $\alpha_H = 0.02(V + 45.8)/\{1 - \exp[-0.15(V + 45.8)]\}$ and $\beta_H = 0.12\exp[-0.057(V + 45.8)]$.

From the solution of Eqs. (4)–(6) in Appendix A, we may write

$$I_{g,2}(t) = \frac{\alpha[\gamma Q_3 - (\alpha+\beta)Q_2]}{(\omega_2-\omega_1)}[\exp(-\omega_1 t) - \exp(-\omega_2 t)] + \frac{\alpha Q_2}{(\omega_2-\omega_1)}[\omega_2\exp(-\omega_1 t) - \omega_1\exp(-\omega_2 t)], \quad (30)$$

and for $t \gg 1/\omega_2$, the high-frequency terms are small when $\omega_2 \gg \omega_1$, and thus

$$I_{g,2}(t) \approx \frac{\alpha\exp(-\omega_1 t)}{(\omega_2-\omega_1)}[\gamma Q_3 + (\omega_2 - \alpha - \beta)Q_2]. \quad (31)$$

If $\alpha \gg \gamma$ and $\beta \gg \delta$, $\omega_1 \approx \alpha_{n,2} + \beta_{n,2}$, $\omega_2 \approx \alpha + \beta$, and

$$I_{g,2}(t) \approx \alpha_{n,2} Q_3 \exp(-\omega_1 t), \quad (32)$$

where $\alpha_{n,2}$ is given by Eq. (17). However, if $\alpha \ll \gamma$ and $\beta \gg \delta$, $\omega_1 \approx \alpha_{n,2} + \beta_{n,2}$, $\omega_2 \approx \gamma + \beta$, and

$$I_{g,2}(t) \approx \alpha_{n,2}[Q_3 + (1 - \alpha/\gamma)Q_2]\exp(-\omega_1 t), \quad (33)$$

where $\alpha_{n,2}$ is given by Eq. (22). That is, for $t \gg 1/\omega_2$, the two-stage expression for the gating current may be approximated by the low-frequency terms, and a similar analysis may also be applied to the domain of a Na^+ ion channel, but in order to account for the rising phase of the gating current that has been observed in both *Shaker* [11] and squid axon K^+ channels [27], as well as Na^+ ion channels [28], it is necessary to take into account the high-frequency contribution.

From Eq. (30),

$$\frac{dI_{g,2}}{dt}(0) = \alpha[\gamma Q_3 - (\alpha+\beta)Q_2], \quad (34)$$

where it is assumed that $Q_2 \approx Q_3$ [11], and for hyperpolarized clamp potentials, $\beta \gg \alpha, \gamma$ and the gating current decreases initially, whereas for depolarized potentials, β is small and an initial rising phase in the relaxation of the gating current is dependent on the relative magnitude of the forward rate functions α and γ. For the two-stage activation model of the squid axon K^+ ion channel, $\alpha \gg \gamma$, and hence $dI_{g,2}/dt(0) < 0$, and there is no rising phase of the gating current for each clamp potential, whereas for the two-stage activation model of the *Shaker* K^+ ion channel for which $\gamma > \alpha$, $dI_{g,2}/dt(0) > 0$, and the gating current has a rising phase for larger depolarizations [11].

Based on the measurement of macroscopic ionic and gating currents and single-channel currents across a K^+ ion channel membrane over a broad voltage range, it has been proposed that the voltage sensor in each of the four subunits is activated through three transitions before ion channel opening [24] and has received support from molecular dynamics simulations of the voltage sensor domain within K^+ ion channels [17–19]. If the S4 voltage sensor is activated in three stages between four states (see Fig. 6), the solution of the Smoluchowski equation for the activation landscape may be expressed as a master equation,

$$\frac{dn_1(t)}{dt} = -\alpha_1 n_1(t) + \beta_1 n_2(t), \quad (35)$$

$$\frac{dn_2(t)}{dt} = \alpha_1 n_1(t) + \beta_2 n_3(t) - (\beta_1 + \alpha_2)n_2(t), \quad (36)$$

$$\frac{dn_3(t)}{dt} = \alpha_2 n_2(t) + \beta_3 n(t) - (\beta_2 + \alpha_3)n_3(t), \quad (37)$$

$$\frac{dn(t)}{dt} = \alpha_3 n_3(t) - \beta_3 n(t), \quad (38)$$

$$n_1 \underset{\beta_1}{\overset{\alpha_1}{\rightleftharpoons}} n_2 \underset{\beta_2}{\overset{\alpha_2}{\rightleftharpoons}} n_3 \underset{\beta_3}{\overset{\alpha_3}{\rightleftharpoons}} n$$

FIG. 6. Three-stage activation model of a K^+ ion channel voltage sensor, where the occupation probabilities of the closed states n_1, n_2, and n_3 and the open state n satisfy a master equation, and α_i, β_i for $i = 1$ to 3 are voltage-dependent rate functions between states.

where the rate functions

$$\alpha_i(V) = \alpha_{i0}\exp[q_{\alpha_i}V/kT], \quad \beta_i(V) = \beta_{i0}\exp[-q_{\beta_i}V/kT], \tag{39}$$

for $i = 1$ to 3, α_{i0} and β_{i0} are constants (ms^{-1}), and q_{α_i} and q_{β_i} are the equivalent charges for the ith forward or backward transition for each stage.

Assuming that the rate functions for the last step of activation of the S4 sensor across the membrane are an order of magnitude smaller than previous steps ($\beta_1,\beta_2 \gg \beta_3$ and $\alpha_1,\alpha_2 \gg \alpha_3$), the master equation may be reduced to (see Appendix A)

$$\frac{dn}{dt} = \alpha_{n,3} - (\alpha_{n,3} + \beta_{n,3})n, \tag{40}$$

where the three-stage expressions for the K^+ channel rate functions (denoted by the subscript "n,3") are

$$\alpha_{n,3}(V) \approx \frac{\alpha_3}{1 + (\beta_2/\alpha_2)(1 + \beta_1/\alpha_1)}, \tag{41}$$

$$\beta_{n,3}(V) \approx \beta_3, \tag{42}$$

which also provide a good fit to the rate functions α_n and β_n for the squid axon K^+ channel, and reduce to the expressions in Eqs. (17) and (18) when $\beta_1 = 0$. However, if it is assumed that the rate functions satisfy $\beta_3 \ll \beta_1,\beta_2$ and $\alpha_1 \ll \alpha_2,\alpha_3$, the master equation may be approximated by Eq. (40), where

$$\alpha_{n,3}(V) \approx \frac{\alpha_1\alpha_3}{\alpha_3 + (\beta_2/\alpha_2)(\alpha_3\beta_1/\beta_2 + \beta_1)}, \tag{43}$$

$$\beta_{n,3}(V) \approx \frac{\beta_3(\alpha_1 + \beta_2(\alpha_1 + \beta_1)/\alpha_2)}{\alpha_3 + (\beta_2/\alpha_2)(\alpha_3\beta_1/\beta_2 + \beta_1)}. \tag{44}$$

For a large depolarizing potential V, $\alpha_{n,3}(V) \approx \alpha_1$ and $\beta_{n,3}(V) \approx \beta_3\alpha_1/\alpha_3$, whereas for a hyperpolarizing potential, $\alpha_{n,3}(V) \approx \alpha_1\alpha_2\alpha_3/(\beta_1\beta_2)$ and $\beta_{n,3}(V) \approx \beta_3$.

For three-stage activation of a voltage sensor, the gating charge $Q_{g,3}(t) = Q_2n_2(t) + (Q_2 + Q_3)n_3(t) + (Q_2 + Q_3 + Q_4)n(t)$, and the gating current

$$I_{g,3}(t) = Q_2\frac{dn_2}{dt} + (Q_2 + Q_3)\frac{dn_3}{dt} + (Q_2 + Q_3 + Q_4)\frac{dn}{dt}. \tag{45}$$

For $t \gg 1/\omega_2$, the high-frequency terms of the solution in Eqs. (A7) are small when $\omega_3 \gg \omega_2 \gg \omega_1$ (see Appendix A) and

$$I_{g,3}(t) \approx \frac{\alpha_1\exp(-\omega_1 t)}{(\omega_2 - \omega_1)(\omega_3 - \omega_1)} \times [g_1(\omega_1)Q_2 + (\alpha_3 + \beta_3 - \omega_1)\alpha_2Q_3 + \alpha_2\alpha_3Q_4]. \tag{46}$$

If $\alpha_1 \gg \alpha_2 \gg \alpha_3$ and $\beta_1 \gg \beta_2 \gg \beta_3$,

$$I_{g,3}(t) \approx \alpha_{n,3}\left[\frac{g_1(\omega_1)}{\alpha_2\alpha_3}Q_2 + Q_4\right]\exp(-\omega_1 t), \tag{47}$$

where $\alpha_{n,3}$ is given by Eq. (41). However, if $\alpha_1 \ll \alpha_3 \ll \alpha_2$ and $\beta_3 \ll \beta_1 \ll \beta_2$,

$$I_{g,3}(t) \approx \alpha_{n,3}\left[\frac{g_1(\omega_1)}{\alpha_2\alpha_3}Q_2 + \left(1 - \frac{\alpha_1}{\alpha_3}\right)Q_3 + Q_4\right]\exp(-\omega_1 t), \tag{48}$$

where $\alpha_{n,3}$ is given by Eq. (43), and for a large depolarizing potential, $g_1(\omega_1)/(\alpha_2\alpha_3) \approx 1$ (see Appendix A), and the gating charge is $\int_0^\infty I_{g,3}(t)dt \approx \Sigma_{i=2}^4 Q_i$.

By taking account of the high-frequency contribution to $I_{g,3}(t)$, it may be shown from Eqs. (35)–(38) and the initial conditions $n(0) = 1$, and $n_1(0) = n_2(0) = n_3(0) = 0$, that

$$\frac{dI_{g,3}}{dt}(0) = \alpha_1[\alpha_2Q_3 - (\alpha_1 + \beta_1)Q_2], \tag{49}$$

and if $\alpha_1 < \alpha_2$ and $Q_2 \approx Q_3$, the gating current has a rising phase for larger depolarizations. As in the case of two-stage activation, the condition $\alpha_1 < \alpha_2$ is consistent with the rate function inequality $\alpha_1 \ll \alpha_2,\alpha_3$ required for the rate function Eqs. (43) and (44).

If a two- and three-stage model of activation of a voltage sensor each reduce to the same rate equation, $\alpha_{n,2}(V) = \alpha_{n,3}(V)$ and $\beta_{n,2}(V) = \beta_{n,3}(V)$, and assuming $\alpha_1\beta_2 \approx \alpha_3\beta_1$, the rate functions $\alpha \approx \alpha_1$, $\delta \approx \beta_3$, $\gamma \approx \alpha_3$, $\beta \approx \beta_2(\alpha_1 + \beta_1)/\alpha_2 \approx (\alpha_3\beta_1 + \beta_1\beta_2)/\alpha_2$, and hence the effective charge $q_\beta \approx q_{\beta_1} + q_{\beta_2} + q_{\alpha_2}$ has contributions from several transitions. From Eq. (48), if $Q_2 = Q_3 = Q_4 \approx e$, we may write $I_{g,3}(t) \approx 3e\alpha_{n,3}\exp(-\omega_1 t)$ for $t \gg 1/\omega_2$, and similarly, if $Q_2 = Q_3 \approx 1.5e$, Eq. (33) reduces to $I_{g,2}(t) \approx 3e\alpha_{n,2}\exp(-\omega_1 t)$, and thus $I_{g,2}(t) \approx I_{g,3}(t)$, and the gating charge per subunit is $\int_0^\infty I_{g,2}(t)dt \approx \int_0^\infty I_{g,3}(t)dt \approx 3e$ for a large depolarizing potential. That is, a three-stage model of activation of a K^+ ion channel sensor may be determined that has the same derived rate functions, survival probability $n(t)$, and slow component of the gating current during a voltage clamp as a two-stage model [11] (see Figs. 7 and 8). The three-stage

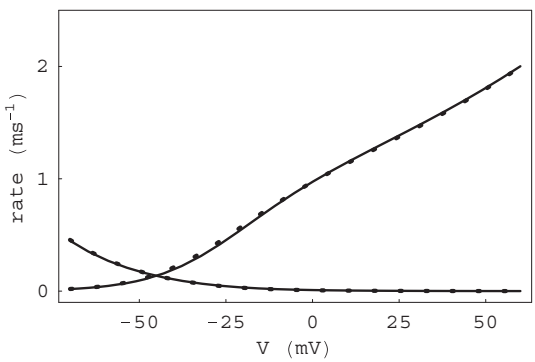

FIG. 7. The derived rate functions $\alpha_{n,2}(V)$ and $\beta_{n,2}(V)$ are calculated for a two-stage K^+ channel (solid line), where $\alpha(V) = 1.1\exp(0.25V/25)$, $\beta(V) = 0.37\exp(-1.6V/25)$, $\gamma(V) = 2.8\exp(0.32V/25)$, $\delta(V) = 0.021\exp(-1.1V/25)$ (ms^{-1}), and $\alpha_{n,3}(V)$, $\beta_{n,3}(V)$ are calculated for a three-stage K^+ ion channel (dotted line), where the rate functions $\alpha_1(V) = 1.1\exp(0.25V/25)$, $\alpha_2(V) = 24.0\exp(0.28V/25)$, $\alpha_3(V) = 4.0\exp(0.28V/25)$, $\beta_1(V) = 1.17\exp(-0.75V/25)$, $\beta_2(V) = 7.0\exp(-0.75V/25)$, $\beta_3(V) = 0.021\exp(-1.1V/25)$.

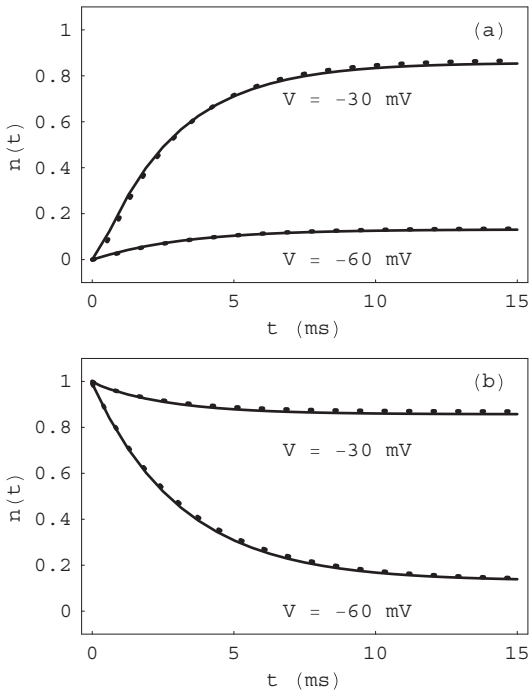

FIG. 8. Survival probability of the state $n(t)$ during a voltage clamp for a two-stage (solid line) and three-stage (dotted line) model of activation of a K^+ ion channel voltage sensor during (a) activation and (b) deactivation, for the rate functions described in the legend of Fig. 7.

rate functions have a similar voltage dependence to those obtained from an electrostatic model of S4 activation [23], where approximately $1e$ is transferred across the membrane for each of the three activation steps per subunit, and provides a good fit to an empirical three-stage model of K^+ channel activation [24].

III. TWO-STAGE K^+ ION CHANNEL SENSOR ACTIVATION AND THE ACTION POTENTIAL

In this section, we consider the effect of two-stage activation of a K^+ channel on potential oscillations across a membrane. The *Shaker* K^+ channel permits the conduction of ions when the activation of each of four voltage sensors through several closed states is followed by a cooperative transition to the open state [11]. However, in order to simplify the analysis, it is initially assumed that (1) the K^+ conductance is modulated by a single S4 sensor that activates in two stages; (2) each ion channel is persistent, that is, does not inactivate; and (3) the activation of the Na^+ channel sensor is instantaneous. More generally, the Na^+ channel has a finite activation time and subsequently inactivates, and K^+ and Na^+ channel conductance are each regulated by several voltage sensors, and therefore, we may compare the effect of two-stage activation of a K^+ channel and the corresponding rate equation on a limit-cycle solution of the HH equations.

The potential response of a membrane with noninactivating Na^+, K^+, and leakage ion channels may be described by the current equation

$$C\frac{dV}{dt} = I - \overline{g}_{\mathrm{Na}} m_\infty(V)(V - V_{\mathrm{Na}}) - \overline{g}_{\mathrm{K}} n(V - V_{\mathrm{K}}) - \overline{g}_L(V - V_L), \tag{50}$$

and the master equation for two-stage activation of the K^+ ion channel sensor

$$\frac{dn}{dt} = \phi_n(V)\left(\frac{1 - n_1}{1 + \rho_n \exp[-(q_\gamma + q_\delta)(V - V_0)/kT]} - n\right), \tag{51}$$

$$\frac{dn_1}{dt} = \phi_1(V)\left(\frac{1 - n}{1 + \rho_1 \exp[(q_\alpha + q_\beta)(V - V_0)/kT]} - n_1\right), \tag{52}$$

where Eq. (5) has been eliminated by application of $n_2 = 1 - n_1 - n$, $\overline{g}_i$ is the maximal ion conductance, and V_i is the equilibrium potential for each ion (Na^+, K^+, and leakage), $\rho_1 = \alpha_0/\beta_0$, $\rho_n = \delta_0/\gamma_0$, $\phi_1(V) = \alpha(V) + \beta(V)$, $\phi_n(V) = \gamma(V) + \delta(V)$, C=1 μF/cm^2. The rate functions for Na^+ channel activation in the squid axon are [1]

$$\alpha_m = \frac{0.1(V + V_m - 25)}{1 - \exp[-0.1(V + V_m - 25)]}, \qquad \beta_m = 4\exp[-(V + V_m)/18], \tag{53}$$

where V_m is a parameter, and the steady-state Na^+ channel open probability is $m_\infty(V) = \alpha_m/(\alpha_m + \beta_m)$, a good approximation to the activation variable m when the Na^+ channel activation time is small.

Based on the effect on Na^+ channel currents of double-cysteine mutants of S4 gating charges and the negative charge E43 on the S1 segment, structural models of resting and activated states of the VSD of the bacterial Na^+ channel NaChBac, which resembles a vertebrate Na_V ion channel domain, demonstrate that at least two transitions occur during activation of each voltage sensor [29]. This conclusion is consistent with a model of the activation of a Na channel based on the measurement of a rising phase of the gating current in a squid axon membrane, and the chemical structure of a Na channel [30]. Therefore, adopting the two-stage expressions in Eqs. (17) and (18) for the Na^+ channel rate functions (denoted by the subscript "m,2"), we may define $\alpha_{m,2} = 2.6\exp[0.28(V + V_m)/25]/\{1 + 8.4\exp[-z_m(V + V_m)/25]\}$, where z_m is a parameter, such that $\alpha_{m,2} \approx \alpha_m$ when $z_m = 1.3$, $\beta_{m,2} = \beta_m$, and $m_\infty(V) \approx \alpha_{m,2}/(\alpha_{m,2} + \beta_{m,2})$. The empirical Na^+ and K^+ ion channel forward rate functions for the squid axon, α_m and α_n, have a similar exponential-quasilinear dependence on V [1] and this may occur when their respective voltage sensors require more than one step to activate, and $q_\alpha \approx q_\gamma \ll q_\beta$.

The stationary points of the system of Eqs. (50)–(52) are given by the intersection of the V, n, and n_1 nullclines, and their stability may be determined from the characteristic equation (see Appendix B). If the two-stage activation of the K^+ ion channel satisfies $\beta \gg \delta$, and $\alpha \gg \gamma$, we may substitute $n_1 = (1 - n)\beta/(\alpha + \beta)$ into Eq. (51) to obtain a rate equation for n, and hence the solutions of Eqs. (14), (17), (18), and (50) provide a good fit to the solutions of

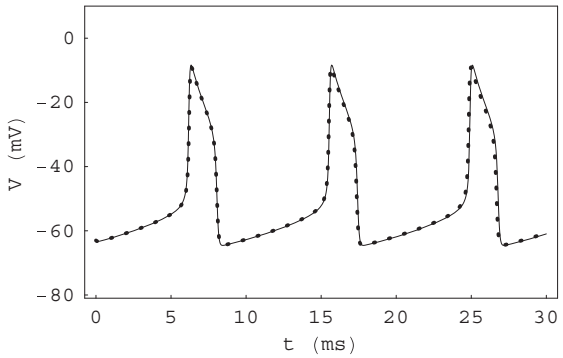

FIG. 9. The limit-cycle solution of Eqs. (50)–(52) (solid line) may be approximated by the solution of Eqs. (14), (17), (18), and (50) (dotted line) when $\beta \gg \delta$ and $\alpha \gg \gamma$. The rate functions $\alpha(V) = 6.4\exp[0.3(V - V_0)/25]$, $\beta(V) = 17.6\exp[-1.4(V - V_0)/25]$, $\gamma(V) = 0.24\exp[0.345(V - V_0)/25]$, $\delta(V) = 0.125\exp[-0.312(V - V_0)/25]$, $\overline{g}_K = 34$ mS/cm^2, $\overline{g}_{Na} = 15$ mS/cm^2, $\overline{g}_L = 0.1$ mS/cm^2, $V_K = -72$ mV, $V_{Na} = 55$ mV, $V_L = -49.4$ mV, $I = 92$ μA/cm^2, $V_0 = -57.9$, $z_m = 1.3$, $V_m = 58$.

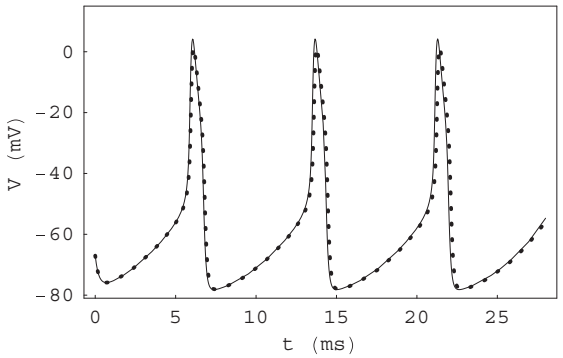

FIG. 11. The limit-cycle solution of Eqs. (50)–(52) (solid line) may be approximated by the solution of Eqs. (14), (50), (54), and (55) (dotted line) when $\beta \gg \delta$ and $\gamma \gg \alpha$. The rate functions $\alpha(V) = 1.1\exp(0.25V/25)$, $\beta(V) = 1.1\exp(-1.6V/25)$, $\gamma(V) = 8.4\exp(0.32V/25)$, $\delta(V) = 0.021\exp(-1.1V/25)$, $\overline{g}_K = 17$ mS/cm^2, $\overline{g}_{Na} = 9$ mS/cm^2, $\overline{g}_L = 0.1$ mS/cm^2, $V_K = -81$ mV, $V_{Na} = 46$ mV, $V_L = -58.4$ mV, $I = 13$ μA/cm^2, $z_m = 1.5$, $V_m = 51.9$.

Eqs. (50)–(52)—see Figs. 9 and 10 for the squid axon K^+ ion channel, where the bifurcation analysis is generated by XPPAUTO [31]. However, if $\beta \gg \delta$, and $\alpha \ll \gamma$, we may substitute $n_2 = (\alpha n_1 + \delta n)/(\beta + \gamma)$ into Eqs. (4) and (6) to obtain Eq. (14), where

$$\alpha_{n,2}(V) \approx \frac{\alpha\gamma}{\alpha + \gamma + \beta}, \tag{54}$$

$$\beta_{n,2}(V) \approx \frac{\delta(\alpha + \beta)}{\alpha + \gamma + \beta}, \tag{55}$$

which reduce to Eqs. (22) and (23) when $\gamma \gg \alpha$, and therefore, the solutions of Eqs. (14), (50), (54), and (55) provide a good fit to the solutions of Eqs. (50)–(52)—see Figs. 11 and 12 for the *Shaker* K^+ ion channel. If $q_\gamma, q_\delta \ll e$, the range of currents for which there is a coexistence of a stable state and a stable limit cycle (bistability) is small (see Fig. 10). However, for larger values of q_δ, similar to measured values for the *Shaker* K^+ ion channel, the range of bistability increases for the bifurcation point HB1 (see Fig. 12), and for values of $q_\alpha \approx q_\gamma$ greater than the normal range for K^+ ion channels ($>0.4e$), there may exist a region of bistability for each bifurcation point.

However, if $\beta \ll \delta$, and $\alpha \ll \gamma$, the variation in the probability n_1 that the sensor occupies the first closed state is an order of magnitude slower than for the variable n, and hence n_1 may be treated as a parameter that modifies the stability of the stationary state in the (V, n) subsystem (see Fig. 13) [32]. During the subthreshold oscillation, from Eq. (52) n_1 increases until the stationary state in the subsystem becomes unstable,

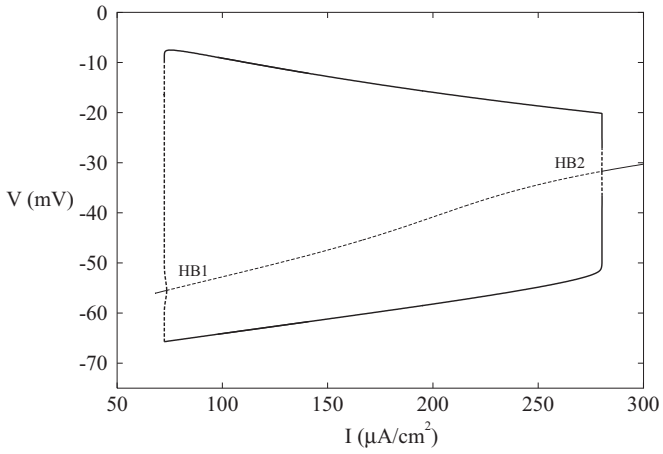

FIG. 10. The bifurcation diagram for Eqs. (50)–(52), when $\beta \gg \delta$ and $\alpha \gg \gamma$, represents the extremal values for the stable periodic solutions (thick solid line), unstable periodic solutions (thick dashed line), and the subcritical bifurcation points HB1 and HB2 at the intersection between stable stationary points (thin solid line) and unstable stationary points (thin dashed line)—see Fig. 9 for a limit-cycle solution.

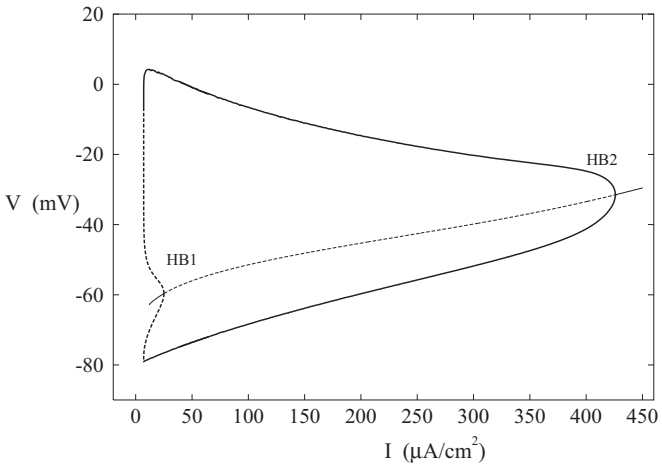

FIG. 12. The bifurcation diagram for Eqs. (50)–(52), when $\beta \gg \delta$ and $\gamma \gg \alpha$, where the subcritical (HB1) and supercritical (HB2) bifurcation points are at the junction between stable stationary points (thin solid line) and unstable stationary points (thin dashed line)—see Fig. 11 for a limit-cycle solution.

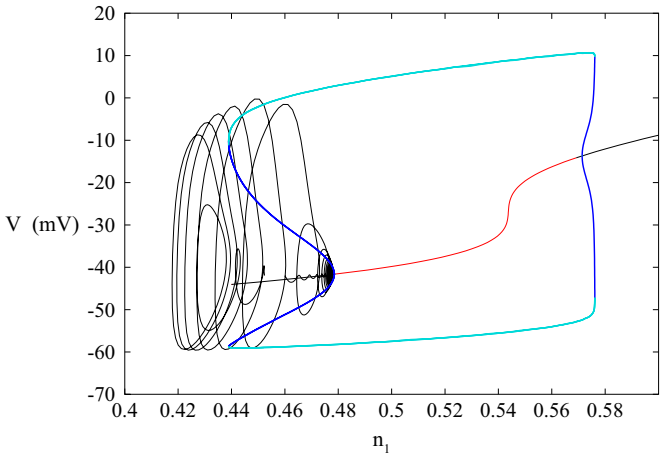

FIG. 13. (Color online) The bifurcation diagram for Eqs. (50) and (51), where $\beta \ll \delta$ and $\alpha \ll \gamma$, the slow variable n_1 is treated as a parameter in the (V, n) subsystem (red and blue line), and the V vs. n_1 projection is computed from Eqs. (50)–(52) (solid line). For n_1 less than 0.48, the stationary point is stable but for n_1 above this value, it is unstable. The rate functions are $\alpha(V) = 0.17\exp(0.5V/25)$, $\beta(V) = 0.02\exp(-V/25)$, $\gamma(V) = 2.8\exp(0.45V/25)$, $\delta(V) = 0.44\exp(-V/25)$, $\alpha_m(V)$, and $\beta_m(V)$ defined by Eq. (53), $V_m = 45$, $\overline{g}_K = 36\ \mathrm{mS/cm^2}$, $\overline{g}_{Na} = 12\ \mathrm{mS/cm^2}$, $\overline{g}_L = 0.4\ \mathrm{mS/cm^2}$, $V_K = -90$ mV, $V_{Na} = 70$ mV, $V_L = -70$ mV, $I = 236\ \mu\mathrm{A/cm^2}$.

and the trajectory spirals toward an action potential burst (see Figs. 13 and 14). However, during the large amplitude oscillation, n_1 progressively decreases until the stationary state is stable and the system returns to equilibrium, followed by a loss of stability as n_1 again increases, and therefore, Eqs. (50)–(52) may exhibit a mixed-mode or bursting oscillation.

Membrane potential oscillations in the squid axon may be described by the HH current equation [1]

$$C\frac{dV}{dt} = I - \overline{g}_{Na}m^3h(V - V_{Na}) - \overline{g}_K n^4(V - V_K) - \overline{g}_L(V - V_L), \tag{56}$$

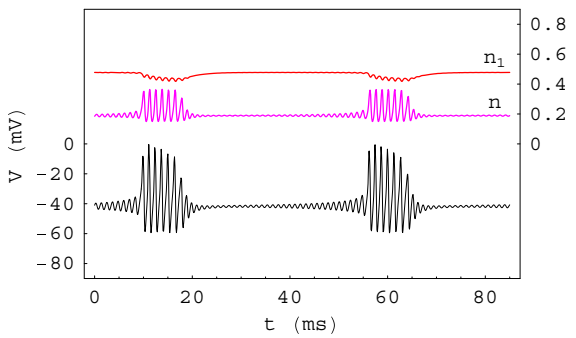

FIG. 14. (Color online) When $\beta \ll \delta$ and $\alpha \ll \gamma$, Eqs. (50)–(52) may exhibit a small amplitude oscillation in V that alternates with a cluster of spikes and is described as a bursting oscillation (see Fig. 13).

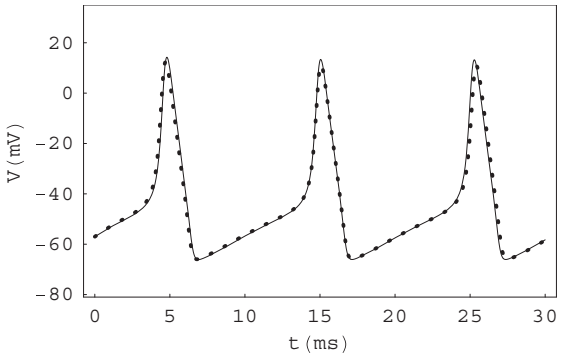

FIG. 15. During a limit-cycle solution of Eqs. (56)–(58), the two-stage activation of K^+ channels, defined by Eqs. (51)–(52) and $\beta \gg \delta$, $\alpha \gg \gamma$ (solid line), may be approximated by a rate equation, Eqs. (14), (17), and (18) (dotted line). The rate functions $\alpha(V) = 6.4\exp[0.3(V - V_0)/25]$, $\beta(V) = 17.6\exp[-1.4(V - V_0)/25]$, $\gamma(V) = 0.24\exp[0.345(V - V_0)/25]$, $\delta(V) = 0.125\exp[-0.312(V - V_0)/25]$, $\alpha_m(V)$ and $\beta_m(V)$ defined by Eq. (53), $V_m = 60$, $\overline{g}_K = 36\ \mathrm{mS/cm^2}$, $\overline{g}_{Na} = 120\ \mathrm{mS/cm^2}$, $\overline{g}_L = 0.3\ \mathrm{mS/cm^2}$, $V_K = -72$ mV, $V_{Na} = 55$ mV, $V_L = -49.4$ mV, $I = 42\ \mu\mathrm{A/cm^2}$, $V_0 = -60$.

where the Na^+ activation variable m and inactivation variable h satisfy the rate equations

$$\frac{dm}{dt} = \alpha_m - (\alpha_m + \beta_m)m, \tag{57}$$

$$\frac{dh}{dt} = \alpha_h - (\alpha_h + \beta_h)h,$$
$$\alpha_h = 0.07\exp[-0.05(V + V_m)], \tag{58}$$
$$\beta_h = \frac{1}{1 + \exp[-0.1(V + V_m - 30)]},$$

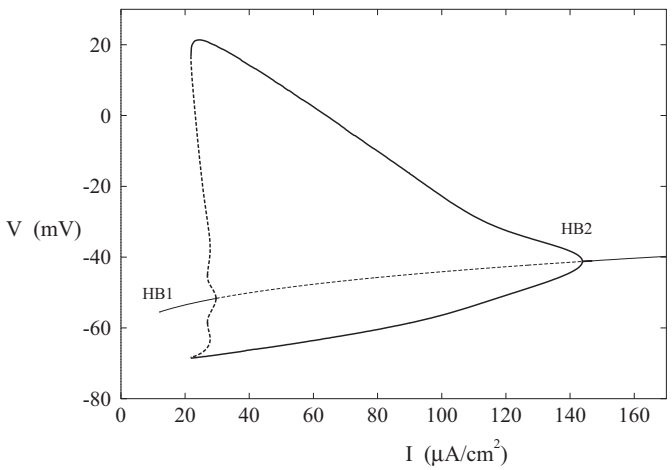

FIG. 16. The bifurcation diagram for Eqs. (51) and (52) and Eqs. (56)–(58), when $\beta \gg \delta$ and $\alpha \gg \gamma$, represents the extremal values for the stable periodic solutions (thick solid line), unstable periodic solutions (thick dashed line), and the subcritical (HB1) and supercritical (HB2) bifurcation points, which occur at the intersection between stable stationary points (thin solid line) and unstable stationary points (thin dashed line)—see Fig. 15 for a limit-cycle solution.

where α_m and β_m are defined in Eq. (53). During a limit-cycle solution of Eqs. (56)–(58) for the squid axon, two-stage activation of the K^+ ion channel may be approximated by a rate equation when $\beta \gg \delta$ and $\alpha \gg \gamma$—see Figs. 15 and 16, and a similar result applies to activation of the *Shaker* K^+ channel when $\beta \gg \delta$ and $\alpha \ll \gamma$.

IV. CONCLUSION

A two-stage model of the activation of a voltage sensor in each of the four subunits of a *Shaker* K^+ ion channel, followed by a cooperative opening transition, can describe the kinetic activation and deactivation of both ionic and gating currents [11] but does not account for the success of the two-state Hodgkin-Huxley model [1]. In this paper, we show that if the rate functions satisfy $\delta \ll \beta$ and either $\alpha \gg \gamma$ or $\gamma \gg \alpha$, the solution of a two-stage model of the activation of an ion channel sensor during a voltage clamp may be approximated by the solution of a rate equation where the backward transition rate is an exponential function of V, and the forward rate may be expressed as an exponential-quasilinear function of V, and have a similar form to the empirical rate functions α_n and β_n of the squid axon K^+ ion channel, and the functions α_x and β_x of a delayed rectifier K^+ ion channel in a cardiac Purkinje fiber [1,25].

The derived rate functions account for the asymmetry of α_n and β_n in terms of the effective charge for the transitions of the activation process, which may be calculated from the voltage-dependence of the barrier heights for each stage of activation of the S4 sensor [23]. If the opening of a K^+ ion channel occurs upon the activation of each of four independent two-stage voltage sensors, the K^+ conductance may be expressed as $\overline{g}_K n^4$, where n is the solution to the corresponding rate equation with derived rate functions $\alpha_{n,2}$ and $\beta_{n,2}$. However, during the voltage clamp of a two-stage opening of a K^+ ion channel, the gating current has a contribution from each transition and exhibits a rising phase for a large depolarization when $\gamma > \alpha$ and, therefore, is in accord with experimental data from *Shaker* [11] and squid axon [27] K^+ ion channels.

If the S4 sensor is activated through three transitions where the first forward transition and the first backward transition are rate limiting ($\alpha_1 \ll \alpha_2,\alpha_3$ and $\beta_3 \ll \beta_1,\beta_2$), the master equation during a voltage clamp also reduces to a rate equation. By expressing a two-stage model of voltage sensor activation as a three-stage model with the same derived rate functions and survival probability for the activated state, it may be shown that an empirical model of K^+ ion channel activation [11] is consistent with models based on the structure of a voltage-sensing domain in which approximately $1e$ is transferred across the membrane for each of the three activation steps per subunit. The rate function inequalities are supported by recent experiments that have shown that the activation time is reduced when the residue V363 adjacent to R1 on the S4 segment and the residue I287 on the S2 segment are replaced by the hydrophilic amino acid Thr [22], and that the deactivation time for the first backward transition is dependent on the hydrophobicity of the residue F^{290} on the S2 segment of a K^+ ion channel subunit [20,21].

Two-stage activation of the K^+ ion channel during an action potential, where the Na^+ ion channel is either persistent or inactivating, may be described by a single variable n when $\delta \ll \beta$ and either $\alpha \gg \gamma$ or $\gamma \gg \alpha$, and therefore is consistent with experimental data for the squid axon K^+ ion channel [1]. However, if $\beta \ll \delta$ and $\alpha \ll \gamma$, the system may exhibit a mixed-mode or bursting oscillation, in which the alternation of repeated spikes with a subthreshold oscillation may be attributed to the modulation of the K^+ conductance by the variation in the occupation probability of the inner closed state n_1.

The interaction between inactivating K^+ ion channels and Na^+ ion channels may also generate bursting in fast spiking cortical neurons but, in this case, deinactivation increases the K^+ conductance until the burst cannot be sustained, and inactivation reduces the K^+ conductance during the quiescent phase enabling another burst of spikes [33,34]. Bursting may also occur when a slow M-type K^+ current modulates the repetitive action potential generated by Na^+ ion channels and delayed rectifier K^+ ion channels, and has been observed in hippocampal CA1 pyramidal neurons [35]. Each of these examples of bursting incorporates an additional variable or ionic current that modifies the stability of the stationary state, but the HH model can exhibit a mixed-mode oscillation when the physiological time constant for either the K^+ channel activation variable n or the Na^+ channel inactivation variable h is increased by an order of magnitude [36,37]. Similarly, the equations that describe the interaction between a persistent Na^+ ion channel and the two-stage opening of a K^+ ion channel have bursting solutions that are suppressed by the parameter values that characterize the K^+ ion channel rate functions.

APPENDIX A

The master equation for two-stage activation, Eqs. (4) to (6), may be expressed as

$$\begin{aligned} \frac{dn_1(t)}{dt} &= -(\alpha+\beta)n_1(t) + \beta[1-n(t)], \\ \frac{dn(t)}{dt} &= \gamma[1-n_1(t)] - (\gamma+\delta)n(t), \end{aligned} \tag{A1}$$

where Eq. (5) has been eliminated by substitution of $n_2 = 1 - n_1 - n$. Assuming that the solution is of the form

$$\begin{aligned} n_1(t) &= n_{1s} + d_1 \exp(-\omega t), \\ n(t) &= n_s + d \exp(-\omega t), \end{aligned}$$

where n_{1s} and n_s are stationary solutions and d_1 and d are constants, the general solution of Eqs. (A1) is

$$\begin{aligned} n_1(t) &= n_{1s} + \sum_{i=1}^{2} a_i(\omega_i - \gamma - \delta)\exp(-\omega_i t), \\ n(t) &= n_s + \gamma \sum_{i=1}^{2} a_i \exp(-\omega_i t), \end{aligned}$$

where $n_{1s} = \beta\delta/[\alpha\gamma + \delta(\alpha+\beta)]$, $n_s = \alpha\gamma/[\alpha\gamma + \delta(\alpha+\beta)]$, ω_1 and ω_2 ($>\omega_1$) are solutions of

$$\omega^2 - \omega(\alpha+\beta+\gamma+\delta) + \alpha\gamma + \delta(\alpha+\beta) = 0, \tag{A2}$$

and a_1,a_2 are constants determined by the initial conditions. For a large hyperpolarized holding potential, we may assume

that $n_1(0) = 1$, and $n(0) = n_2(0) = 0$, and if a K^+ channel voltage sensor is depolarized to a clamp potential V, by application of the initial condition, the solution of Eqs. (4)–(6) for two-stage activation is

$$\begin{aligned} n_{1A}(t) &= \frac{\beta\delta}{\omega_1\omega_2} - \frac{\alpha(\gamma+\delta-\omega_1)}{\omega_1(\omega_1-\omega_2)}\exp(-\omega_1 t) \\ &\quad + \frac{\alpha(\gamma+\delta-\omega_2)}{\omega_2(\omega_1-\omega_2)}\exp(-\omega_2 t), \\ n_{2A}(t) &= \frac{\alpha\delta}{\omega_1\omega_2} - \frac{\alpha(\omega_1-\delta)}{\omega_1(\omega_1-\omega_2)}\exp(-\omega_1 t) \\ &\quad + \frac{\alpha(\omega_2-\delta)}{\omega_2(\omega_1-\omega_2)}\exp(-\omega_2 t), \\ n_A(t) &= \frac{\alpha\gamma}{\omega_1\omega_2} + \frac{\alpha\gamma}{\omega_1(\omega_1-\omega_2)}\exp(-\omega_1 t) \\ &\quad - \frac{\alpha\gamma}{\omega_2(\omega_1-\omega_2)}\exp(-\omega_2 t). \end{aligned} \tag{A3}$$

However, if the S4 sensor is initially in the open state [$n(0) = 1$, and $n_1(0) = n_2(0) = 0$], and if the K^+ sensor is repolarized to a clamp potential V, the solution is

$$\begin{aligned} n_{1D}(t) &= \frac{\beta\delta}{\omega_1\omega_2} - \frac{\beta\delta}{\omega_1(\omega_2-\omega_1)}\exp(-\omega_1 t) \\ &\quad - \frac{\beta\delta}{\omega_2(\omega_1-\omega_2)}\exp(-\omega_2 t), \end{aligned} \tag{A4}$$

$$\begin{aligned} n_{2D}(t) &= \frac{\alpha\delta}{\omega_1\omega_2} + \frac{\delta(\omega_1-\alpha)}{\omega_1(\omega_2-\omega_1)}\exp(-\omega_1 t) \\ &\quad + \frac{\delta(\omega_2-\alpha)}{\omega_2(\omega_1-\omega_2)}\exp(-\omega_2 t), \end{aligned} \tag{A5}$$

$$\begin{aligned} n_D(t) &= \frac{\alpha\gamma}{\omega_1\omega_2} + \frac{\delta(\omega_2-\gamma-\delta)}{\omega_1(\omega_2-\omega_1)}\exp(-\omega_1 t) \\ &\quad + \frac{\delta(\omega_1-\gamma-\delta)}{\omega_2(\omega_1-\omega_2)}\exp(-\omega_2 t). \end{aligned} \tag{A6}$$

Assuming that the solution of the three-stage master equation, Eqs. (35)–(38), is of the form

$$\begin{aligned} n_i(t) &= n_{is} + d_i\exp(-\omega t), \\ n(t) &= n_s + d\exp(-\omega t), \end{aligned}$$

for $i = 1,3$, the general solution is

$$\begin{aligned} n_1(t) &= \frac{\beta_1\beta_2\beta_3}{\omega_1\omega_2\omega_3} + \alpha_1\Sigma_{i=1}^3 a_i g_1(\omega_i)\exp(-\omega_i t), \\ n_2(t) &= \frac{\alpha_1\beta_2\beta_3}{\omega_1\omega_2\omega_3} - \alpha_1\Sigma_{i=1}^3 a_i g_2(\omega_i)\exp(-\omega_i t), \\ n_3(t) &= \frac{\alpha_1\alpha_2\beta_3}{\omega_1\omega_2\omega_3} - \alpha_1\alpha_2\Sigma_{i=1}^3 a_i(\beta_3-\omega_i)\exp(-\omega_i t), \\ n(t) &= \frac{\alpha_1\alpha_2\alpha_3}{\omega_1\omega_2\omega_3} - \alpha_1\alpha_2\alpha_3\Sigma_{i=1}^3 a_i\exp(-\omega_i t), \end{aligned} \tag{A7}$$

where a_1, a_2, and a_3 are constants, $g_1(\omega) = \omega^2 - (\alpha_2 + \alpha_3 + \beta_2 + \beta_3)\omega + \alpha_2(\alpha_3 + \beta_3) + \beta_2\beta_3$, $g_2(\omega) = \omega^2 - (\alpha_3 + \beta_2 + \beta_3)\omega + \beta_2\beta_3$, the frequencies $\omega_1 < \omega_2 < \omega_3$ are solutions of

$$\omega^3 - e_1\omega^2 + e_2\omega - e_3 = 0, \tag{A8}$$

and

$$\begin{aligned} e_1 &= \Sigma_{i=1}^3(\alpha_i + \beta_i) = \Sigma_{i=1}^3\omega_i \\ e_2 &= \alpha_1(\alpha_2 + \alpha_3 + \beta_2 + \beta_3) + \alpha_2(\alpha_3 + \beta_3) + \beta_2\beta_3 \\ &\quad + \beta_1(\alpha_3 + \beta_2 + \beta_3) \\ &= \omega_1\omega_2 + \omega_2\omega_3 + \omega_1\omega_3 \\ e_3 &= \alpha_1\alpha_2\alpha_3 + \beta_3[\alpha_1\alpha_2 + \beta_2(\alpha_1 + \beta_1)] = \omega_1\omega_2\omega_3. \end{aligned}$$

If the K^+ channel voltage sensor is depolarized to a clamp potential V from a hyperpolarized potential [$n_1(0) = 1$, and $n(0) = n_2(0) = n_3(0) = 0$], it may be shown that $a_i = 1/[\omega_i\Pi_{j\neq i}(\omega_j - \omega_i)]$, for $i = 1$ to 3. Assuming $\alpha_1 \geqslant \alpha_2 \gg \alpha_3$ and $\beta_1 \geqslant \beta_2 \gg \beta_3$, we may write

$$\omega_2 + \omega_3 \approx \Sigma_{i=1}^2(\alpha_i + \beta_i), \tag{A9}$$

$$\omega_2\omega_3 \approx \alpha_1\alpha_2 + \alpha_1\beta_2 + \beta_1\beta_2, \tag{A10}$$

$$\omega_1 = \alpha_{n,3} + \beta_{n,3} = \frac{e_3}{\omega_2\omega_3}, \tag{A11}$$

and if, in addition, $\alpha_1 \gg \alpha_2$ and $\beta_1 \gg \beta_2$, it follows that $\omega_3 \approx \alpha_1 + \beta_1$, $\omega_2 \approx \alpha_1\alpha_2/(\alpha_1 + \beta_1) + \beta_2$, $\omega_1 \ll \omega_2 \ll \omega_3$ and $a_1 \gg a_2 \gg a_3$. That is, the higher-frequency terms have small amplitude and $n(t)$ satisfies a rate equation with time constant $\omega_1 = \alpha_{n,3}(V) + \beta_{n,3}(V)$, where

$$\begin{aligned} \alpha_{n,3}(V) &\approx \frac{\alpha_3}{1 + (\beta_2/\alpha_2)(1 + \beta_1/\alpha_1)}, \\ \beta_{n,3}(V) &\approx \beta_3. \end{aligned}$$

However, assuming $\alpha_1 \ll \alpha_2,\alpha_3$ and $\beta_3 \ll \beta_1,\beta_2$,

$$\begin{aligned} \omega_2 + \omega_3 &\approx \Sigma_{i=1}^2(\alpha_{i+1} + \beta_i), \\ \omega_2\omega_3 &\approx \alpha_3\alpha_2 + \alpha_3\beta_1 + \beta_1\beta_2, \end{aligned}$$

and if $\alpha_2 \gg \alpha_3$ and $\beta_2 \gg \beta_1$, we may write $\omega_3 \approx \alpha_2 + \beta_2$, $\omega_2 \approx (\alpha_2\alpha_3 + \alpha_3\beta_1 + \beta_1\beta_2)/(\alpha_2 + \beta_2)$, $a_1 \gg a_2 \gg a_3$, and the rate functions

$$\alpha_{n,3}(V) \approx \frac{\alpha_1\alpha_3}{\alpha_3 + (\beta_2/\alpha_2)(\alpha_3\beta_1/\beta_2 + \beta_1)}, \tag{A12}$$

$$\beta_{n,3}(V) \approx \frac{\beta_3(\alpha_1 + \beta_2(\alpha_1 + \beta_1)/\alpha_2)}{\alpha_3 + (\beta_2/\alpha_2)(\alpha_3\beta_1/\beta_2 + \beta_1)}. \tag{A13}$$

APPENDIX B

Stationary points of the system of Eqs. (50)–(52) are given by the intersection of the n, n_1, and V nullclines—$n = (1 - n_1)\gamma/(\gamma + \delta)$, $n_1 = (1 - n)\beta/(\alpha + \beta)$ and

$$n = \frac{I - \overline{g}_L(V - V_L) - \overline{g}_{Na}m_\infty(V)(V - V_{Na})}{\overline{g}_K(V - V_K)}, \tag{B1}$$

and hence

$$\frac{I-\overline{g}_L(V-V_L)-\overline{g}_{\rm Na}m_\infty(V)(V-V_{\rm Na})}{\overline{g}_{\rm K}(V-V_{\rm K})}=\frac{\alpha\gamma}{\alpha\gamma+\alpha\delta+\beta\delta}, \tag{B2}$$

where it is assumed that the parameters are chosen so that there is only one solution. The stability of the stationary point may be determined by assuming that $V=V_s+\widetilde{V}, n=n_s+\widetilde{n}$, and $n_1=n_{1s}+\widetilde{n}_1$, where (V_s,n_s,n_{1s}) is the stationary solution, and defining the Jacobian matrix of coefficients M of the linearized equations in $(\widetilde{V},\widetilde{n},\widetilde{n}_1)$,

$$M=\begin{pmatrix} R & -g_{\rm K}(V_s-V_{\rm K})/C & 0 \\ \phi_{ns}n'_{\infty s}(1-n_{1s}) & -\phi_{ns} & -\phi_{ns}n_{\infty s} \\ \phi_{1s}n'_{1\infty s}(1-n_s) & -\phi_{1s}n_{1\infty s} & -\phi_{1s} \end{pmatrix}, \tag{B3}$$

where $R=[-g_L-g_{\rm K}n_s-g_{\rm Na}m_{\infty s}-g_{\rm Na}m'_\infty(V_s)(V_s-V_{\rm Na})]/C$, $n_\infty(V)=\gamma/(\gamma+\delta)$, $n_{1\infty}(V)=\beta/(\alpha+\beta)$, $\phi_{ns}=\phi_n(V_s),\phi_{1s}=\phi_1(V_s),n_{\infty s}=n_\infty(V_s),n_{1\infty s}=n_{1\infty}(V_s)$, $n'_{\infty s}=n'_\infty(V_s)$, $n'_{1\infty s}=n'_{1\infty}(V_s)$, and $m_{\infty s}=m_\infty(V_s)$, the eigenvalues may be determined from the characteristic equation

$$\det(M-I\omega)=\omega^3+f_1\omega^2+f_2\omega+f_3=0, \tag{B4}$$

where I is the identity matrix, and

$$\begin{aligned} f_1&=\phi_{ns}+\phi_{1s}-R,\\ f_2&=-R(\phi_{ns}+\phi_{1s})-\phi_{ns}\phi_{1s}(1-n_{\infty s}n_{1\infty s})\\ &\quad+(g_{\rm K}/C)(V_s-V_{\rm K})\phi_{ns}n'_{\infty s}(1-n_{1s}),\\ f_3&=(g_{\rm K}/C)(V_s-V_{\rm K})\phi_{ns}\phi_{1s}\\ &\quad\times[n'_{\infty s}(1-n_{1s})-n_{\infty s}n'_{1\infty s}(1-n_s)]\\ &\quad+R\phi_{ns}\phi_{1s}(n_{\infty s}n_{1\infty s}-1). \end{aligned}$$

[1] A. L. Hodgkin and A. F. Huxley, J. Physiol. **117**, 500 (1952).
[2] D. Noble, J. Physiol. **160**, 317 (1962).
[3] B. Frankenhaeuser and A. F. Huxley, J. Physiol. **171**, 302 (1964).
[4] J. A. Connor and C. F. Stevens, J. Physiol. **213**, 31 (1971).
[5] R. E. Plant and M. Kim, Biophysical J. **16**, 227 (1976).
[6] I. Goychuk and P. Hänggi, Proc. Natl. Acad. Sci. U.S.A. **99**, 3552 (2002).
[7] S. R. Vaccaro, Phys. Rev. E **76**, 011923 (2007).
[8] S. R. Vaccaro, Phys. Rev. E **78**, 061915 (2008).
[9] H. Lecar, H. P. Larsson, and M. Grabe, Biophys. J. **85**, 2854 (2003).
[10] S. R. Vaccaro, J. Chem. Phys. **132**, 145101 (2010).
[11] W. N. Zagotta, T. Hoshi, and R. W. Aldrich, J. Gen. Physiol. **103**, 321 (1994).
[12] S. K. Tiwari-Woodruff, M. A. Lin, C. T. Schulteis, and D. M. Papazian, J. Gen. Physiol. **115**, 123 (2000).
[13] W. R. Silverman, B. Roux, and D. M. Papazian, Proc. Natl. Acad. Sci. U.S.A. **100**, 2935 (2003).
[14] D. Schmidt, Q. X. Jiang, and R. MacKinnon, Nature **444**, 775 (2006).
[15] V. Jogini and B. Roux, Biophys. J. **93**, 3070 (2007).
[16] F. Khalili-Araghi, V. Jogini, V. Yarov-Yarovoy, E. Tajkhorshid, B. Roux, and K. Schulten, Biophys. J. **98**, 2189 (2010).
[17] U. Henrion, J. Renhorn, S. I. Borjesson, E. M. Nelson, C. S. Schwaiger, P. Bjelkmar, B. Wallner, and E. Lindahl, Proc. Natl. Acad. Sci. U.S.A. **109**, 8552 (2012).
[18] L. Delemotte, M. Tarek, M. L. Klein, C. Amaral, and W. Treptow, Proc. Natl. Acad. Sci. U.S.A. **108**, 6109 (2011).
[19] M. O. Jensen, V. Jogini, D. W. Borhani, A. E. Leffler, R. O. Dror, and D. E. Shaw, Science **336**, 229 (2012).
[20] X. Tao, A. Lee, W. Limapichat, D. A. Dougherty, and R. MacKinnon, Science **328**, 67 (2010).
[21] J. L. Lacroix and F. Bezanilla, Proc. Natl. Acad. Sci. U.S.A. **108**, 6444 (2011).
[22] J. L. Lacroix, F. V. Campos, L. Frezza, and F. Bezanilla, Neuron **79**, 651 (2013).
[23] S. R. Vaccaro, J. Chem. Phys. **135**, 095102 (2011).
[24] N. E. Schoppa and F. J. Sigworth, J. Gen. Physiol. **111**, 271 (1998).
[25] D. DiFrancesco and D. Noble, Phil. Trans. R. Soc. Lond. B **307**, 353 (1985).
[26] B. Roux, Biophys. J. **73**, 2980 (1997).
[27] M. M. White and F. Bezanilla, J. Gen. Physiol. **85**, 539 (1985).
[28] C. M. Armstrong and W. F. Gilly, J. Gen. Physiol. **74**, 691 (1979).
[29] P. G. DeCaen, V. Yarov-Yarovoy, T. Scheuer, and W. A. Catterall, Proc. Natl. Acad. Sci. U.S.A. **108**, 18825 (2011).
[30] R. D. Keynes, Proc. R. Soc. Lond. B **240**, 425 (1990).
[31] B. Ermentrout, *Simulating, Analyzing, and Animating Dynamical Systems: A Guide to XPPAUT for Researchers and Students* (SIAM, Philadelphia, 2002).
[32] J. Rinzel, Lect. Notes Biomath. **71**, 267 (1987).
[33] X.-J. Wang, Neuroreport **5**, 221 (1993).
[34] M. E. Rush and J. Rinzel, Bull. Math. Biol. **57**, 899 (1995).
[35] C. Yue and Y. Yaari, J. Neuroscience **24**, 4614 (2004).
[36] S. Doi, S. Nabetani, and S. Kumagai, Biol. Cybern. **85**, 51 (2001).
[37] J. Rubin and M. Wechselberger, Biol. Cybern. **97**, 5 (2007).